Analysis of cancellation in two-dimensional magnetohydrodynamic turbulence

L. Sorriso-Valvo, V. Carbone, A. Noullez, H. Politano, A. Pouquet, and P. Veltri

Citation: Physics of Plasmas (1994-present) **9**, 89 (2002); doi: 10.1063/1.1420738
View online: http://dx.doi.org/10.1063/1.1420738
View Table of Contents: http://scitation.aip.org/content/aip/journal/pop/9/1?ver=pdfcov
Published by the AIP Publishing

Analysis of cancellation in two-dimensional magnetohydrodynamic turbulence

L. Sorriso-Valvo[a)]
Dipartimento di Fisica and Istituto di Fisica della Materia, Università della Calabria, Rende (CS), Italy and Lab. Cassini, Observatoire de la Côte d'Azur, Nice, France

V. Carbone
Dipartimento di Fisica and Istituto di Fisica della Materia, Università della Calabria, Rende (CS), Italy

A. Noullez and H. Politano
Lab. Cassini, Observatoire de la Côte d'Azur, Nice, France

A. Pouquet
ASP/NCAR, P.O. Box 3000, Boulder, Colorado 80307

P. Veltri
Dipartimento di Fisica and Istituto di Fisica della Materia, Università della Calabria, Rende (CS), Italy

(Received 9 July 2001; accepted 20 September 2001)

A signed measure analysis of two-dimensional intermittent magnetohydrodynamic turbulence is presented. This kind of analysis is performed to characterize the scaling behavior of the sign-oscillating flow structures, and their geometrical properties. In particular, it is observed that cancellations between positive and negative contributions of the field inside structures are inhibited for scales smaller than the Taylor microscale, and stop near the dissipative scale. Moreover, from a simple geometrical argument, the relationship between the cancellation exponent and the typical fractal dimension of the structures in the flow is obtained. © *2002 American Institute of Physics.* [DOI: 10.1063/1.1420738]

I. INTRODUCTION

Self-similarity is a signature of complex flows with strong nonlinearities. Huge amounts of effort have been deployed in determining scaling laws of energy spectra and, more generally speaking, of structure functions (see, e.g., Refs. 1 and 2), both in geophysical and astrophysical flows, in the laboratory and using numerical simulations as well. Nonlinear behavior of the scaling exponents is generally interpreted as due to the presence of strong localized structures both in space and time. Indeed, structures have been observed in turbulent flows for a long time: sheets, spirals, and filaments of vorticity both in the incompressible[3–6] and compressible case,[7] in the latter with shocks as well. In magnetohydrodynamics (MHD), current and vorticity sheets seem to prevail in three dimensions[8–13] whereas in two-dimensional space, current and vorticity filaments are the main identifiable structures.[14–16] Such features are locally complex, with rapid fluctuations corresponding to flux cancellations, in three dimensions[10] as well as in two dimensions, and as first strikingly observed in chaotic dynamos using mappings;[17] in such cases, very high Reynolds number flows can be modeled and cancellations of flux occur at all scales, leading to a very complex magnetic field.

We study in this paper the geometrical properties of the vorticity and current fields (as well as their combination through the Elsässer variables defined in the following). The data stem from a direct numerical simulation in two space dimensions and our study focuses on the computation of the cancellation exponent introduced by Ott *et al.*[17] These exponents allow for a simple characterization of the flows and can be linked to the fractal dimension of the typical structures.

The present paper is organized as follows. In Sec. II, we recall the definitions of the signed measure and cancellation exponent. In Sec. III, we describe the data stemming from a numerical simulation, and the main features of the fields are characterized by the typical scales of the flow. Section IV describes the results obtained from the analysis of the cancellation properties of our flow. In Sec. V, we introduce a simple model, based on geometrical arguments, which connect the cancellation exponent to the fractal dimension of the structures. Our results are discussed and the main conclusions of the paper are re-emphasized in Sec. VI.

II. THE SIGNED MEASURE AND THE CANCELLATION EXPONENT

Intermittency in turbulent fields is related to the presence of structures at different scales. The proximity of such structures may lead to rapid changes of sign in the fields derivatives. In order to describe the scaling properties of sign oscillations, Ott *et al.*[17] introduced the concept of *sign-singular measures*. In analogy to probability measures (positive definite), the signed measure of a zero-mean scalar field $f(\mathbf{r})$, defined on a set $Q(L)$ of size L, can be introduced in the d-dimensional case. Let $\{Q_i(l)\}\subset Q(L)$ be a hierarchy of

a)Electronic mail: sorriso@obs-nice.fr

disjoint subsets of size l covering $Q(L)$. Then, for each scale l and for each set of boxes $Q_i(l)$, the signed measure is defined as

$$\mu_i(l)=\frac{\int_{Q_i(l)}d\mathbf{r}\,f(\mathbf{r})}{\int_{Q(L)}d\mathbf{r}|f(\mathbf{r})|}. \tag{1}$$

The choice of the normalization factor [the denominator in Eq. (1)] will be justified in the following. The signed measure thus can be interpreted as the difference between two probability measures, one for the positive part and the other for the negative part of the field.[18]

As the scale of the subset $Q_i(l)$ increases, cancellations between opposite sign structures, and then between the two probability measures, come into play. This feature can be characterized by investigating the scaling properties of the partition function:

$$\chi(l)=\sum_{Q_i(l)}|\mu_i(l)|, \tag{2}$$

where the sum is extended to all disjoint subset $Q_i(l)$. It is clear that if $\mu_i(l)$ is a probability measure, as well as if the field is defined in sign, the choice of the normalization factor in (1) leads to $\chi(l)=1$. On the other hand, if cancellations are present, we can expect that their effect is less and less important as the scale l decreases, so that $\chi(l)$ increases. In the latter case, we can investigate the scaling behaviors of the weakness of cancellations by a scaling exponent κ, defined through $\chi(l)\sim l^{-\kappa}$, where κ is called the *cancellation exponent*. This exponent represents a quantitative measure of the cancellation efficiency. Furthermore, if this scaling law exists, in analogy with the singularities of probability measures, the signed measure is called sign singular. If the field is smooth, then trivially $\kappa=0$. It can be shown that for homogeneous fields with discontinuities, $\kappa=1$, whereas for stochastic processes $\kappa=d/2$,[19] d being the dimensionality of the space. More generally, as will be shown in Sec. VI, if the field $\mathbf{f}(\mathbf{r})$ is homogeneous with a Hölder scaling exponent h, that is if $\langle\|\Delta\mathbf{f}(\mathbf{l})\|\rangle=\langle\|\mathbf{f}(\mathbf{r}+\mathbf{l})-\mathbf{f}(\mathbf{r})\|\rangle\sim l^h$, then $\kappa=h$.[19,20] This relation between the cancellation exponent and scaling exponents can be generalized to higher order partition functions and structure functions $S_p(l)=\langle\Delta^{\parallel}\mathbf{f}(l)^p\rangle\sim l^{\zeta_p}$ (where $\Delta^{\parallel}\mathbf{f}(\mathbf{l})=[\mathbf{f}(\mathbf{r}+\mathbf{l})-\mathbf{f}(\mathbf{r})]\cdot\hat{\mathbf{l}}$ defines the longitudinal increments of $\mathbf{f}$ on scale l) to determine the generalized dimensions of the set where the singularities of the field f live.[19,21]

Besides the work of Ott *et al.*[17] on fast magnetic dynamos, several flows in the context of plasma turbulence have been examined using such concepts, in order to characterize the oscillating features of turbulent fields. For example, the magnetic helicity in the solar wind has been shown to be sign singular,[22] and solar photospheric velocity patterns[23] as well. Finally, the variations of the cancellation exponent of the current helicity between the pre- and postflare periods for major H-α solar flares, have been used to evidence variations in the heliospheric magnetic field structures of active regions.[24]

III. THE NUMERICAL SIMULATION AND THE TYPICAL SCALES OF THE FLOW

The data we analyze with the technique described in Sec. II stem from a numerical simulation of the two-dimensional ($d=2$) magnetohydrodynamics (MHD) equations written below in terms of the Elsässer variables $\mathbf{z}^{\pm}=\mathbf{v}\pm\mathbf{b}$:

$$(\partial_t+\mathbf{z}^{\mp}\cdot\boldsymbol{\nabla})\mathbf{z}^{\pm}=-\boldsymbol{\nabla}P_*+\nu^{\pm}\nabla^2\mathbf{z}^{\pm}+\nu^{\mp}\nabla^2\mathbf{z}^{\mp}+\mathbf{F}^{\pm}, \tag{3}$$

where P_* is the total pressure, $2\nu^{\pm}=\nu\pm\eta$, ν being the viscosity and η the magnetic diffusivity, while $\mathbf{F}^{\pm}$ are the forcing terms. The incompressibility conditions $\boldsymbol{\nabla}\cdot\mathbf{z}^{\pm}=0$ complete the equations.

The MHD equations have nonlinear scaling properties so that Kolmogorov-type arguments[25] can be performed to evaluate dimensionally the scaling properties of structure functions, but taking into account the specificity of MHD flows. The less efficient interaction rate between the $\mathbf{z}^{\pm}$ structures may well lead to scaling laws that differ from the classical Kolmogorov case, as first derived in the so-called Iroshnikov–Kraichnan phenomenology[26] for globally isotropic flows (i.e., in the absence of a strong uniform magnetic field $\mathbf{B}_0$ at zero frequency), a phenomenology which takes into account the presence of Alfvénic fluctuations in the plasma. Small-scale intermittency is present in MHD as in the fluid case, and is related to the presence of coherent structures which locally in space obviously break the isotropy assumption. However, in the Kolmogorov spirit, isotropy is recovered on average. The effects of these structures on the phenomenology for MHD flows have been pointed out and discussed in several ways (see, e.g., Refs. 10 and 27).

In the present paper, we want to analyze the oscillating character of such structures, and their geometrical properties. Equation (3) is solved with a pseudospectral method on a grid of 1024^2 points, with 2π-periodic boundary conditions. The forcing terms $\mathbf{F}^{\pm}$ maintain constant the Fourier modes $\mathbf{k}$ with $|\mathbf{k}|=1$. The magnetic Prandtl number $\mathrm{Pr}=\nu/\eta$ is unity, so that $\nu^{\pm}=\nu=\eta=8\times10^{-4}$. The correlations between the velocity and the magnetic field lead initially to $\rho_C=2\langle\mathbf{v}\cdot\mathbf{b}\rangle/\langle|\mathbf{v}|^2+|\mathbf{b}|^2\rangle\sim6\%$. The time-averaged Reynolds number is $\mathrm{Re}\sim1600$ and the integral scale is $l_0/L=0.25\pm0.02$, where $L=2\pi$ is the size of the computational box. Further details about the simulation can be found in Refs. 28 and 29. In the present work, we analyze ten samples separated by approximately 16 eddy turnover times once all transients have died out and a statistically steady state has been reached.

A snapshot of the current is shown in Fig. 1. The top picture shows the local accumulation of sheets, probably through folding, whereas the bottom picture clearly reveals the oscillating character of the flow structures. The analysis of the probability distribution functions (PDFs) of the field fluctuations,[29] and of the scaling exponents of the structure functions[28] has revealed that both the Elsässer fields, as well as the magnetic field and the velocity, are strongly intermittent, as already visualized in earlier computations.[15,14] This intermittency is already quite evident when one computes the flatness factor $F(s)=\langle[\Delta^{\parallel}\mathbf{f}(s)]^4\rangle/\langle[\Delta^{\parallel}\mathbf{f}(s)]^2\rangle^2$ that goes

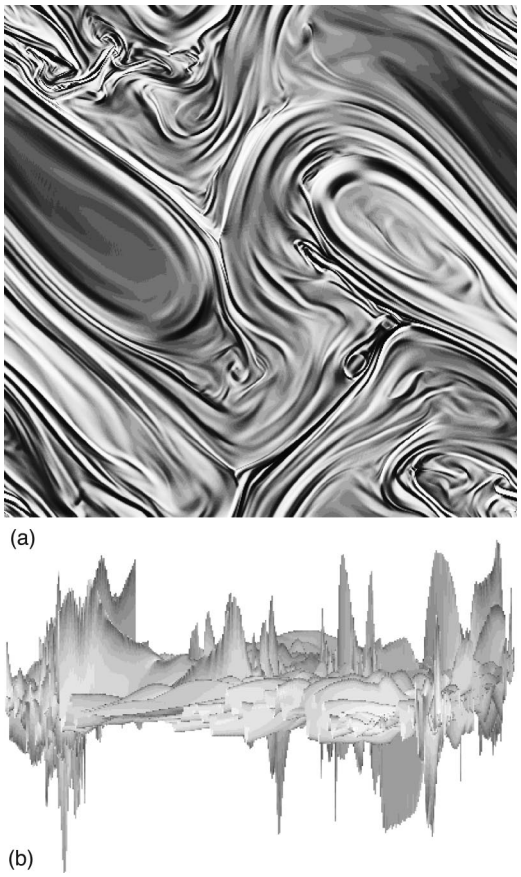

FIG. 1. A snapshot of the current J at time $t=7.3$ in gray levels (top), and a pseudo-3D perspective view of the same field (bottom) showing the existence of structures of different signs at all scales.

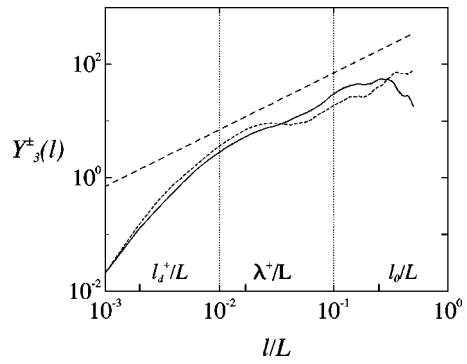

FIG. 2. The time averaged third-order correlators $Y_3^+(l)$ (continuous line) and $Y_3^-(l)$ (dashed line) in a log–log plot. The straight line is a simple linear law, and is displayed as reference. The dissipation scale l_d^+, the Taylor microscale λ^+, and the integral scale l_0 are indicated, as well as the bounds of the inertial range.

from the Gaussian value 3 at large scales s for all fields, to values $F\sim 40$ for $\mathbf{f}\equiv\mathbf{v}$, $F\sim 80$ for $\mathbf{f}\equiv\mathbf{b}$, $F\sim 65$ for $\mathbf{f}\equiv\mathbf{z}^{\pm}$ at the smallest resolved scale. This dramatic change in flatness reflects the change in shape of the PDFs through the scales, as quantified in Ref. 29.

Following Politano and Pouquet,[30] it can be shown that the third-order correlators defined in the following obey, in the inertial range, the following scaling law in dimension d:

$$Y_3^{\pm}(l)=\langle \Delta^{\parallel}\mathbf{z}^{\mp}(l)\|\Delta\mathbf{z}^{\pm}(l)\|^2\rangle=-\frac{4}{d}\epsilon^{\pm}l, \tag{4}$$

where $\Delta\mathbf{z}^{\pm}(l)=\mathbf{z}^{\pm}(\mathbf{r}+\mathbf{l})-\mathbf{z}^{\pm}(\mathbf{r})$ is the vector increment of the field $\mathbf{z}^{\pm}$, and $\Delta^{\parallel}$ is its (scalar) longitudinal projection; thus, the flux functions $Y_3^{\pm}(l)$ involve all components of the physical fields. The coefficient $\epsilon^{\pm}$ are the mean energy transfer rates of the $\mathbf{z}^{\pm}$ variables. We recall that in the framework of the Kolmogorov phenomenology, the mean energy transfer rate is assumed to be equal to the mean energy injection rate, as well as to the mean energy dissipation rate. In order to estimate $\epsilon^{\pm}$, the data are fitted for each time in the ranges where relation (4) is verified. Averaging in time in order to decrease statistical errors, we evaluate $\epsilon^{+}\sim 550$ and $\epsilon^{-}\sim 440$. The difference between the two $\pm$ rates is linked to the correlation between the velocity and the magnetic field, and should increase with increasing ρ_C and disappear only in the limit of vanishing ρ_C. Figure 2 displays the $Y_3^{\pm}(l)$ third-order correlators. It appears that the exact scaling law (4)—obtained in the limit of very large Reynolds numbers, otherwise correction terms not written here would arise due to dissipation—is better verified in the case of Y_3^+ than for Y_3^-, where the scaling range coincides with the inertial range as determined in Ref. 28 (see the following). Note that, because the fluxes are odd order in the fields, cancellations occur that render scaling laws difficult to unravel. For that reason, it is customary to estimate the inertial range by computing the modified third-order correlators, taking absolute values to obtain $L_3^{\pm}(l)=\langle|\Delta^{\parallel}\mathbf{z}^{\mp}(l)|\|\Delta\mathbf{z}^{\pm}(l)\|^2\rangle\sim l$. This leads to an inertial range extending from 0.01 to 0.1 in l/L for both correlators.[28] The difference in scaling quality between the plus and minus third-order correlators, or higher order moments of the $\mathbf{z}^{+}$ and $\mathbf{z}^{-}$ fields, has already been observed, even when using absolute moments to reduce statistical errors.[13,27,28] This asymmetry between $\mathbf{z}^{+}$ and $\mathbf{z}^{-}$ could be due to a significant role of the velocity-magnetic field correlations on the dynamics of MHD flows, even when $\rho_C\sim 0$. Indeed, the local $\mathbf{v}\cdot\mathbf{b}$, not positive definite, is known to develop strong fluctuations (see, e.g., Ref. 31), precluding identical behavior for $\mathbf{z}^{\pm}$ fields.

We can use the values of $\epsilon^{\pm}$ computed from the law (4) to estimate—in the framework of the IK phenomenology[26]—the typical scales of the flow, i.e., the dissipative scales $l_d^{\pm}=(\nu^2 B_0/\epsilon^{\pm})^{1/3}$ and the Taylor microscales $\lambda^{\pm}=(2\nu E^{\pm}/\epsilon^{\pm})^{1/2}$. Here B_0 represents the rms large-scale magnetic field, and $E^{\pm}$ are the energies associated with the Elsässer fields, which are the ideal invariants of the flow, together with the $\langle a^2\rangle$ correlation, where $\mathbf{b}=\nabla\times\mathbf{a}$ with $\mathbf{a}$ the magnetic potential. The computed scales we obtain are given in Table I, and indicated in the horizontal axis of Fig. 2 as well. In MHD turbulence, it is not possible to unambiguously define directly from the dissipation rates, the Taylor and the dissipative scales for the magnetic and velocity fields independently. However, using several assumptions, namely (i) equipartition, i.e., $\langle\mathbf{v^2}\rangle/2\sim\langle\mathbf{b^2}\rangle/2$ for the kinetic and magnetic energies, (ii) weak total correlation, $\langle\mathbf{v}\cdot\mathbf{b}\rangle\sim 0$, and (iii) unit magnetic Prandtl number, $\mathrm{Pr}\sim 1$, one can then define a dissipation scale $l_d=(\nu^2 B_0/\epsilon)^{1/3}$ and a Taylor microscale $\lambda=(2\nu E/\epsilon)^{1/2}$, where E stands for the total energy, and ϵ for

TABLE I. Estimated values for the typical scales of the flow (see the text for definitions), the cancellation exponents, and the fractal dimensions of the structures for the four fields, averaged on ten temporal snapshots; l_d is the dissipation scale, λ the Taylor scale, l_* denotes the end of the inertial range, and l_S is the saturation scale.

Field	$l_d/L\times10^3$	$\lambda/L\times10^3$	$l_S/L\times10^3$	$l_\star/L\times10^3$	κ	D
J	⋯	⋯	5.0 ± 0.8	15	0.43 ± 0.06	1.14 ± 0.12
ω	⋯	⋯	6.9 ± 1.0	20	0.69 ± 0.12	0.62 ± 0.24
ω^+	2.1 ± 0.7	17 ± 9	5.4 ± 1.0	15	0.50 ± 0.06	1.00 ± 0.12
ω^-	2.4 ± 0.7	18 ± 8	5.4 ± 1.0	15	0.50 ± 0.07	1.00 ± 0.12

its mean transfer and dissipation rates. Doing so, and noting that $\epsilon=(\epsilon^+ + \epsilon^-)/2$, we obtain $l_d/L=(2.2\pm0.4)\times10^{-3}$ and $\lambda/L=1.5\pm0.4\times10^{-2}$. These scales are very close to the ones computed for the Elsässer fields. We are thus left to use $l_d^\pm$ and $\lambda^\pm$ as the typical scales of the flow to refer to.

IV. SCALING PROPERTIES OF THE SIGNED MEASURE IN THE NUMERICAL DATA

We now analyze the scaling properties of the signed measure for the numerical data described previously. As in Sec. III for the evaluation of the energy transfer rates, we do so separately for the different snapshots of the simulation, and we report only the computed averages, while the error bars give an estimate of the dispersion of such values.

We first define the signed scalar densities we need from the physical variables $\mathbf{v}$, $\mathbf{b}$, and $\mathbf{z}^\pm$. For two-dimensional MHD flows, it is convenient to use the rotational of these variables. Indeed, using the Stokes theorem, the circulation of the magnetic field along any closed contour is equal to the normal flux of the current crossing the corresponding surface $Q_i(l)$, $\oint_{C_i(l)}\mathbf{b}(\mathbf{r})\cdot d\ell = \int_{Q_i(l)}\mathbf{J}(\mathbf{r})\cdot\hat{\mathbf{n}}\,d\sigma$. The sign of the current density flux is determined by the clockwise or counterclockwise circulation of the magnetic field. In a two-dimensional geometry, the magnetic field lies in the (x,y) plane, namely $\mathbf{b}(x,y)=(b_x,b_y,0)$, and the current density $\mathbf{J}(x,y)=\boldsymbol{\nabla}\times\mathbf{b}(x,y)$ is along the z direction, perpendicular to the plane. The normal current flux density is then simply $\mathbf{J}\cdot\hat{\mathbf{n}}\,d\sigma=J_z(x,y)\,dx\,dy$, so that $J_z(x,y)\equiv J(x,y)$ can be used as our scalar density. The same argument holds for the vorticity $\boldsymbol{\omega}$ and for $\boldsymbol{\omega}^\pm=\boldsymbol{\omega}\pm\mathbf{j}$, the rotationals of the Elsässer fields. We show in Fig. 3 the coarse-grained current density flux for four different values of the box size l, at one particular time ($t=7.3\sim45\,\tau_{\mathrm{NL}}$, where τ_{NL} is the eddy turnover time once the statistically steady state is reached). As can be seen, strong oscillating signed structures appear at all scales, and cancellation effects clearly increase with the box size. In Fig. 4 we present the function $\chi^J(l)$, computed in the case of the current $J(x,y)$ at each time and averaged over the ten temporal fields we analyze. A clear scaling range is visible, so that a cancellation exponent $\kappa^J=0.43$ can be obtained by performing a least-squares fit of the type

$$\chi(l)=C\left(\frac{l}{L}\right)^{-\kappa}. \tag{5}$$

We now try to relate the scales which characterize the cancellations to the typical scales of the flow itself, namely the Taylor microscales $\lambda^\pm$ and the dissipative ones $l_d^\pm$. The scaling range is determined by looking at the local slope of $\chi^J(l)$ (not shown), and extends from $l_\star^J=0.015L$ to $l_u^J=0.12L$. As can be observed, the range in which the scaling (5) holds is mostly embedded within the inertial range of the flow, given in Sec. III. For scales larger than l_u, the partition function still decays as a power law, but with a larger exponent, approaching the typical behavior expected for a completely uncorrelated point field, with $\kappa=d/2=1$, but the poor statistics at such large scales prevent us from discussing that behavior any further. For scales smaller than $l_\star$, the partition function slowly saturates at the asymptotic value $\chi(l)=1$. The scale l_S, at which the saturation can be considered achieved, is computed as the intersection scale between the power-law (5) and the limit value $\chi(l)=1$, giving $l_S^J=0.005L$ for the current. It is worth pointing out that, due to the choice of normalization in the signed measure, for any dataset with a finite resolution $l_{\min}$, the partition function will trivially go to unity at that scale. The fact that, in our case, saturation of $\chi(l)$ persists for scales larger than $l_{\min}$, demonstrates that the field is well resolved and thus regular at the resolution of the numerical simulation. The departure from a constant behavior of $\chi(l)$ (with $\kappa=0$), occurs only at some yet larger scale, which can be identified as the smallest characteristic scale of the structures which develop in the flow. Typically, we find that the saturation scale l_S is of order of 2–3 times the relevant Kolmogorov scale l_d, showing that the extent of structures in their smallest dimension is controlled by dissipative effects. On the other hand, power-law scaling sets in at the scale $l_\star$ which is found to be of the same order as the Taylor microscale λ. This point can be understood by a simple geometrical argument developed in Sec. V. All these results obtained for the current are confirmed for the other fields ω, ω^+, and ω^-. The values of the cancellation exponents and those of the typical scales related to the partition function for all fields are reported in Table I. It can be observed that the rotationals of the Elsässer fields both present the same behavior, while different values of the parameters are found for the vorticity and the current. Note also that the range of fit for the vorticity is shorter than those for the others fields (not shown).

The higher value of κ^ω reveals that the presence of structures inhibit the cancellations in a less efficient way for the vorticity than for the other fields. Conversely, the current structures inhibit cancellations more efficiently than all other fields.

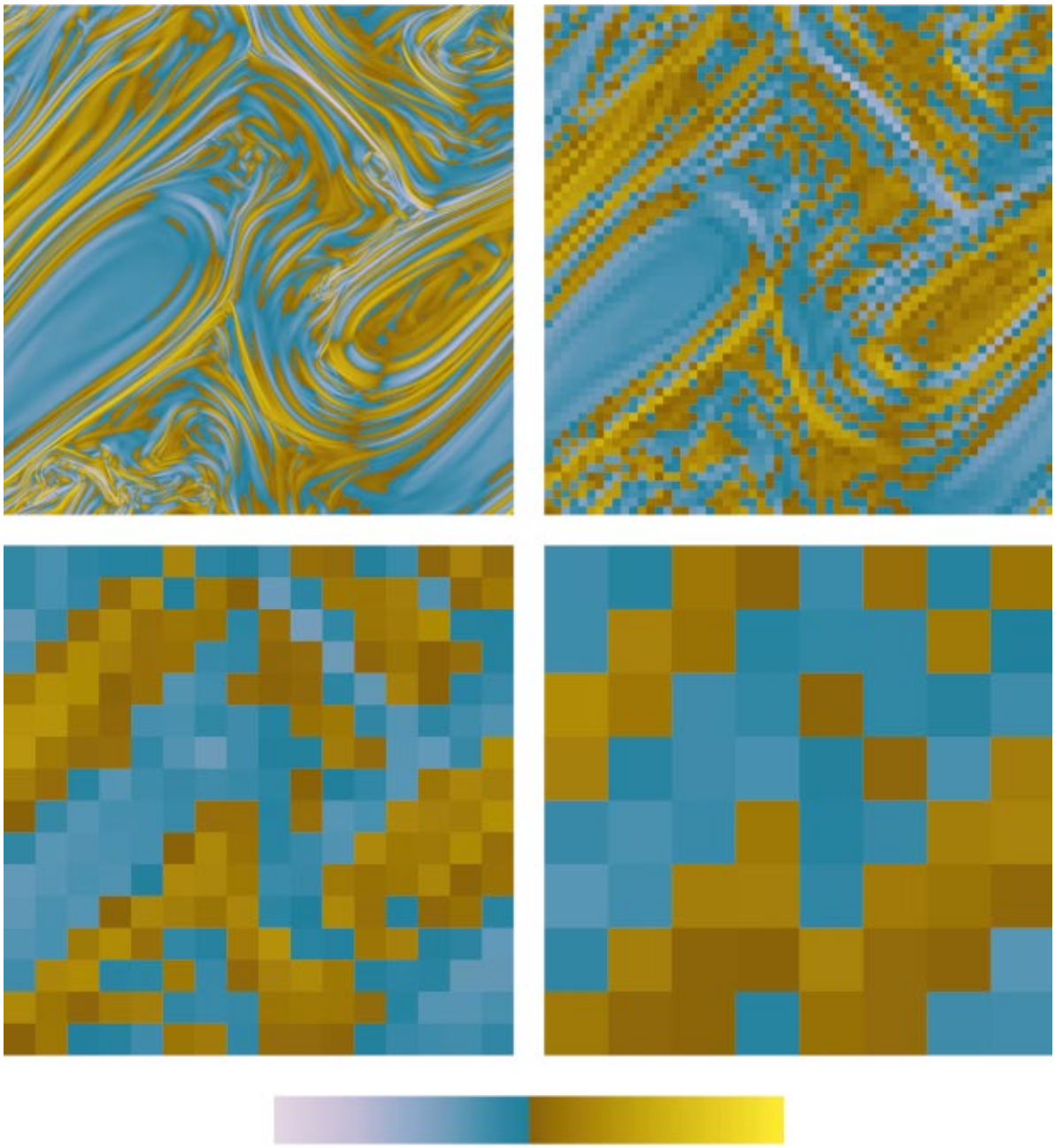

FIG. 3. (Color) The coarse-grained signed measure of the current J at time $t=7.3$ for four different box sizes, namely $l/L=0.001$, $l/L=0.016$, $l/L=0.059$, $l/L=0.12$, from top to bottom. Colors range from cyan for negative J values to yellow for positive ones, going through blue and brown. Cancellations at large scales are responsible for the decrease in magnitude of the measure.

V. CANCELLATION EXPONENTS AND DIMENSIONS OF STRUCTURES

It is clear that cancellation exponents characterize in some way the geometry of structures, as exemplified by the fact that a smooth (continuous) field will give a zero cancellation exponent, while a field made of uncorrelated point-like objects will have a cancellation exponent $\kappa=d/2$. In order to quantify the transition between these two limits, we will use a simple geometrical model that we now introduce.

The relevant Taylor scale λ gives us a mean scale over which a field is correlated. However, it does not tell us the geometry of the structures present at that scale. These could be correlated in some directions for scales much larger than λ, and/or already uncorrelated in some other directions. Let us now assume that the field is smooth (correlated) in D dimensions with a cutoff scale of λ, and uncorrelated in the other $d-D$ dimensions. Of course, if the field becomes completely regular below some scale l_S, the corresponding dimension at that scale will be $D=d$. On the other hand, if structures have some largest extent l_u, the field will consist of isolated, and thus nearly uncorrelated, objects, showing an apparent dimension $D=0$. In the intermediate region, over

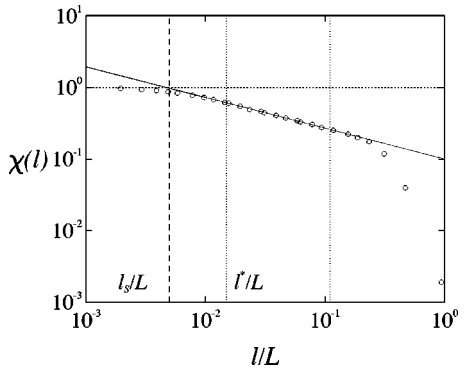

FIG. 4. For the current J, the log–log plot of $\chi(l)$ (averaged over ten snapshots) vs the subsets size l/L. The solid line represents the best fit with the power-law (5). The constant value $\chi_S(l)=1$ is plotted (the horizontal dashed line), and the saturation scale $l_S/L=0.005$ is indicated by the vertical dashed line on the left-hand side. The vertical dotted lines indicate the range of the fit, which lies between $l_\star/L=0.015$ and $l_1/L=0.12$.

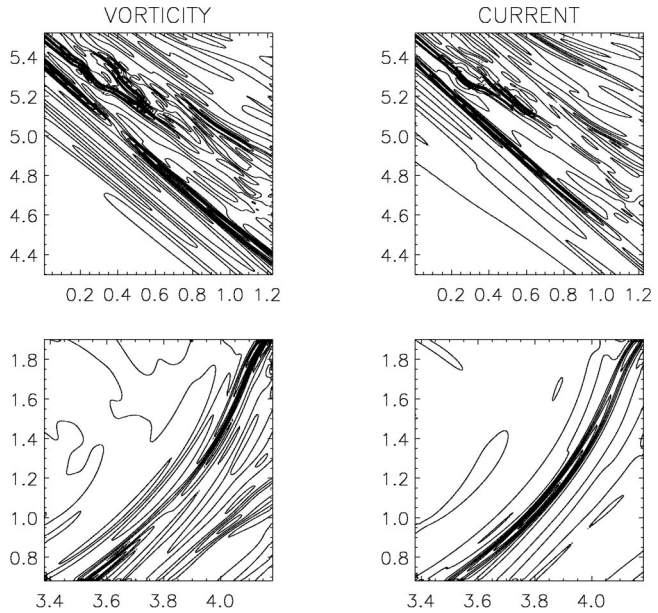

FIG. 5. Examples of contour lines of vorticity (left panel) and current (right panel) structures, at the time $t=6.3$ (top) and $t=6.93$ (bottom). The axes indicate the location of the snapshots within the 2π-periodic box.

which the topology of the structures will have an effect, the partition function of the current J for example, or of any component of a field in dimension d, can be written as

$$\chi(l)=\sum_{Q_i(l)}\left|\frac{\int_{Q_i(l)}d\mathbf{r}\,J(\mathbf{r})}{\int_{Q(L)}d\mathbf{r}|J(\mathbf{r})|}\right| \sim\frac{1}{L^d J_{\rm rms}}\left(\frac{L}{l}\right)^d\left|\int_{Q(l)}d\mathbf{r}\,J(\mathbf{r})\right|, \tag{6}$$

where homogeneity is used to replace the sum over all subsets $Q_i(l)$ by $(L/l)^d$ times the integral over a generic box $Q(l)$ of size l. Moreover, we have approximated the field absolute value integral by its typical value $L^d J_{\rm rms}$. Indeed, because of the absolute values, no cancellations can occur in the denominator. Now, the integral on the subset $Q(l)$ can be done by integrating over regular domains of size λ^d and splitting the number of contributions between the correlated dimensions and the uncorrelated ones. The smooth dimensions will give a contribution proportional to their area $(l/\lambda)^D$. The uncorrelated dimensions will behave like the integral of an uncorrelated field, giving a value proportional to the square root of their area, that is $(l/\lambda)^{(d-D)/2}$. Collecting all contributions, we see that $\chi(l)$ will behave as

$$\chi(l)\sim\frac{\lambda^d J_{\rm rms}}{L^d J_{\rm rms}}\left(\frac{L}{l}\right)^d\left(\frac{l}{\lambda}\right)^D\left(\frac{l}{\lambda}\right)^{(d-D)/2} \sim\left(\frac{l}{\lambda}\right)^{-(d-D)/2}\sim\left(\frac{l}{\lambda}\right)^{-\kappa}. \tag{7}$$

The cancellation exponent can thus be interpreted as half the codimension of the flow structures, $\kappa=(d-D)/2$. Note that this interpretation remains valid at small scales where $\kappa=0$ when $D=d$ and at scales larger or similar to the integral scale where $\kappa=d/2$ when $D=0$.

Specializing to our case with $d=2$, the value of $\kappa^\pm=0.5$ that we found indicates that structures are similar to filaments $D^\pm=1.0\pm0.12$ for the $\boldsymbol{\omega}^\pm$ fields. This result for the Elsässer variables rotationals extends the previous observation of sheet-like structures for the current in three-dimensional MHD,[10,12,13] having a corresponding signature of filaments in two-dimensional cuts.

The current displays a slightly smaller cancellation exponent, that leads to a dimension of 1.14 ± 0.12, which can be interpreted by observing that the current structures are slightly fatter than filaments and show some thickness, likely due to reconnection taking place within current sheets.

The vorticity field has a significantly larger cancellation exponent, that would give a dimension for structures $D^\omega=0.62\pm0.24$, smaller than the one of a filament structure. In fact, a close inspection in physical space shows that vorticity structures, although globally thin and elongated, are more complex than those of the current field (see plots at $t=6.3\sim26\,\tau_{\rm NL}$, and at $t=6.93\sim39\,\tau_{\rm NL}$ in Fig. 5). For example, as already known,[31,32] quadrupole vorticity structures are associated with quasilinear current sheets in the simplest reconnection configuration. This could explain the smaller dimension found for the vorticity structures characterizing what can be seen as a ''disrupted filament.''

VI. CONCLUSION AND DISCUSSION

In order to characterize the oscillating behavior of the dynamical structures present in conductive turbulent flows, we perform a signed measure analysis of data obtained from direct numerical integration of the two-dimensional MHD equations. We obtain that the measure is sign singular, with a clear scaling range for the cancellations between the structures, either for the current and the vorticity field, or for the rotational of the Elsässer variables. The cancellations are inhibited for scales smaller than the Taylor scales while they stop near the dissipative scales. Note that the correspondence—as displayed in Table I—between the typical scales for cancellation and those of the turbulent fluid are

obtained in the framework of MHD flows presenting a weak correlation between the velocity and the magnetic fields and for a magnetic Prandtl number of unity.

Moreover, by a simple geometrical argument, we link the cancellation exponent evaluated here to the fractal dimension of the structures in the flow. This gives us information about the topology of the structures. This interpretation can in fact also be extended. Indeed, the partition function is only a first-order moment, and is thus unable to distinguish, for example, between a regular behavior over some fractal set, and a self-similar behavior over the whole space, as well as intermediate situations. The distinction could only be made by looking at higher order moments.[19] This point is left for future study. But we can already generalize the geometrical argument given in Sec. V to the case where the field is not locally smooth, by introducing a single local scaling exponent h such that (specializing to the magnetic field) $\|\Delta J(s)\| \sim s^{h-1}$ on the structures of dimension D. Note that, because of the presence of structures, h is *not* the exponent of the first-order structure function of J, the latter containing contributions both of structures and background. In this picture, the last integral in expression (6) becomes

$$\int_{Q(l)} d_S^d J(\mathbf{s}) = J_{\mathrm{rms}} \int_{Q(l)} d_S^D \left(\frac{s}{\lambda}\right)^{h-1} \int_{Q(l)} d_S^{d-D}$$

$$= J_{\mathrm{rms}} \lambda^D \left(\frac{l}{\lambda}\right)^{D+h-1} \lambda^{d-D} \left(\frac{l}{\lambda}\right)^{(d-D)/2}$$

$$= \lambda^d J_{\mathrm{rms}} \left(\frac{l}{\lambda}\right)^{D+h-1} \left(\frac{l}{\lambda}\right)^{(d-D)/2},$$

giving a cancellation exponent $\kappa = (d-D)/2 + (1-h)$. In general, as we already pointed out, it is impossible to separate the contributions of the two terms, unless one makes further hypotheses.

Let us consider the particular case of a space filling object ($D=d$) which would not be smooth at small scales, that is with a Hölder self-similarity exponent h smaller than one. The cancellation exponent of its rotational would then be simply $\kappa = 1-h$. Note that if the object is smooth, with $h=1$, this is consistent with $\kappa = 0$ obtained from (7). On the other hand, if the field values are completely independent, we find $\kappa = 1$, that can be easily checked by direct numerical simulations.[23] Using this interpretation, in the case of the velocity rotational that has a cancellation exponent $\kappa = 0.69 \pm 0.12$, we are led to infer a Hölder exponent for the velocity $h = 0.31 \pm 0.12$, close to the Kolmogorov value 1/3 for the velocity field of a neutral turbulent flow. This argument is clearly incomplete because of the presence of structures in the fields, which are even more conspicuous for the rotationals of the magnetic and Elsässer fields. Higher resolution simulations allowing the computation of the full spectrum of higher order cancellation exponents will be necessary to disentangle the contributions of geometry and differentiability to the intermittency of MHD turbulence.

ACKNOWLEDGMENTS

The numerical simulations were performed at IDRIS (Orsay). We received partial financial support from the CNRS Program PNST.

[1] U. Frisch, *Turbulence* (Cambridge University Press, Cambridge, 1995).
[2] K. R. Sreenivasan and R. A. Antonia, Annu. Rev. Fluid Mech. **29**, 435 (1997).
[3] E. Siggia, J. Fluid Mech. **107**, 375 (1981).
[4] W. T. Ashurst, A. R. Kerstein, R. M. Kerr, and C. H. Gibson, Phys. Fluids **30**, 2343 (1987).
[5] Z. S. She, E. Jackson, and S. A. Orszag, Nature (London) **344**, 226 (1990).
[6] A. Vincent and M. Meneguzzi, J. Fluid Mech. **225**, 1 (1991).
[7] D. Porter, A. Pouquet, and P. Woodward, Phys. Rev. Lett. **68**, 3156 (1992).
[8] A. Nordlund, A. Brandenburg, R. L. Jennings, M. Rieutord, J. Ruokolainen, R. F. Stein, and I. Tuominen, Astrophys. J. **392**, 647 (1992).
[9] A. Brandenburg, I. Procaccia, and D. Segel, Phys. Plasmas **2**, 1148 (1995).
[10] H. Politano, A. Pouquet, and P. L. Sulem, Phys. Plasmas **2**, 2931 (1995).
[11] K. Galsgaard and A. Nordlund, J. Geophys. Res., [Atmos.] **102**, 231 (1997).
[12] R. M. Kerr and A. Brandenburg, Phys. Rev. Lett. **83**, 1155 (1999).
[13] D. Biskamp and W. C. Müller, Phys. Plasmas **7**, 4889 (2000).
[14] D. Biskamp and H. Welter, Phys. Fluids B **1**, 1964 (1989).
[15] H. Politano, A. Pouquet, and P. L. Sulem, Phys. Fluids B **1**, 2330 (1989).
[16] H. Friedel, R. Grauer, and C. Marliani, J. Comput. Phys. **134**, 190 (1997).
[17] E. Ott, Y. Du, K. R. Sreenivasan, A. Juneja, and A. K. Suri, Phys. Rev. Lett. **69**, 2654 (1992).
[18] P. R. Halmos, *Measure Theory* (Springer, New York, 1974).
[19] S. I. Vainshtein, K. R. Sreenivasan, R. T. Pierrehumbert, V. Kashyap, and A. Juneja, Phys. Rev. E **50**, 1823 (1994).
[20] A. L. Bertozzi and A. B. Chhabra, Phys. Rev. E **49**, 4716 (1994).
[21] S. I. Vainshtein, Y. Du, and K. R. Sreenivasan, Phys. Rev. E **49**, R2521 (1994).
[22] V. Carbone and R. Bruno, Astrophys. J. **488**, 482 (1997).
[23] G. Consolini, V. Carbone, F. Berrilli *et al.*, Astron. Astrophys. **344**, L33 (1999).
[24] V. I. Abramenko, V. B. Yurkishin, and V. Carbone, Astron. Astrophys. **334**, L57 (1998).
[25] A. N. Kolmogorov, Dokl. Akad. Nauk SSSR **30**, 9 (1941).
[26] P. Iroshnikov, Sov. Astron. **7**, 566 (1963); R. H. Kraichnan, Phys. Fluids **8**, 1385 (1965).
[27] T. Gomez, H. Politano, and A. Pouquet, Phys. Fluids **11**, 2298 (1999).
[28] H. Politano, A. Pouquet, and V. Carbone, Europhys. Lett. **43**, 516 (1998).
[29] L. Sorriso-Valvo, V. Carbone, P. Veltri, H. Politano, and A. Pouquet, Europhys. Lett. **51**, 520 (2000).
[30] H. Politano and A. Pouquet, J. Geophys. Lett. **25**, 273 (1998).
[31] H. Politano, P. L. Sulem and A. Pouquet, in *Topological Fluid Mechanics*, edited by H. K. Moffatt and A. Tsinober (Cambridge University Press, 1990), p. 315.
[32] W. H. Matthaeus, Geophys. Res. Lett. **9**, 660 (1982).